PERGAMON

International Journal of Solids and Structures 40 (2003) 6369–6388

INTERNATIONAL JOURNAL OF SOLIDS and STRUCTURES

www.elsevier.com/locate/ijsolstr

Stress concentrations in the particulate composite with transversely isotropic phases

V.I. Kushch *

Institute for Superhard Materials of the National Academy of Sciences, 2 Avtozavodskaya Str., Kiev 04074, Ukraine

Received 3 March 2003; received in revised form 2 July 2003

Abstract

The accurate series solution have been obtained of the elasticity theory problem for a transversely isotropic solid containing a finite or infinite periodic array of anisotropic spherical inclusions. The method of solution has been developed based on the multipole expansion technique. The basic idea of method consists in expansion the displacement vector into a series over the set of vectorial functions satisfying the governing equations of elastic equilibrium. The re-expansion formulae derived for these functions provide exact satisfaction of the interfacial boundary conditions. As a result, the primary spatial boundary-value problem is reduced to an infinite set of linear algebraic equations. The method has been applied systematically to solve for three models of composite, namely a single inclusion, a finite array of inclusions and an infinite periodic array of inclusions, respectively, embedded in a transversely isotropic solid. The numerical results are presented demonstrating that elastic properties mismatch, anisotropy degree, orientation of the anisotropy axes and interactions between the inclusions can produce significant local stress concentration and, thus, affect greatly the overall elastic behavior of composite.

Keywords: Composite materials; Spherical inclusions; Transversely isotropic materials; Linear elasticity; Multipole expansion; Stress concentrations

1. Introduction

Evaluation of the stress caused by the mismatch in elastic properties of matrix and inhomogeneities is one of the key problems in composite mechanics. Indeed, given the stress and strain fields in the bulk of composite material one can integrate them to determine the macroscopic response, or ''effective'' elastic properties. On the other hand, information on stress concentration, i.e. location and magnitude of peak microstress, provides the necessary basis on which the composite's strength theories can be built up.

For the particulate composites with isotropic constituents, there is a variety of models and methods to evaluate both the stress state and macroscopic elastic moduli. When the volume fraction of disperse phase is

* Tel./fax: +380-444329544.
E-mail address: vkushch@bigmir.net (V.I. Kushch).

0020-7683/$ - see front matter © 2003 Published by Elsevier Ltd.
doi:10.1016/S0020-7683(03)00399-8

low, even simple one-particle models based on the well-known Lame and Eshelby's solutions give a reasonable approximation of stress fields in and around the inclusions. With the volume content increasing, interaction between the disperse phase particles exerts more and more pronounced effect on the composite's behavior. To account for this effect properly, the models of two or more interacting inclusions in a solid should be considered. Various accurate and approximate methods to analyze the many-particle models were proposed by Moskovidis and Mura (1975), Chen and Acrivos (1978), Rodin and Hwang (1991), Hori and Nemat-Nasser (1993) and Kushch (1996), among others. The higher dispersion volume content is, the more sophisticated models and methods are to be applied to predict the composite's behavior. One widely used approach consists in considering the periodic model structure with a periodicity cell containing from one to several particles. This model is advantageous in that it provides a natural way, through the periodic boundary conditions on the opposite cell facets, to account for interactions among a whole infinite array of inhomogeneities. The periodic composite with rigid spherical particles was studied by Nunan and Keller (1984) by the method of singular integral equations, with the elastic ones by Kushch (1985) and Sangani and Lu (1987) who used the multipole expansion method. For the composites with more general ellipsoidal shape of particles an approximate solution for the effective moduli has been obtained by Iwakuma and Nemat-Nasser (1983). Kushch (1997b) has considered more realistic structural model of composite and developed an accurate analytical, multipole expansion-based method of solution. In the last work, the microstress concentrations were investigated as well.

By contrast with the isotropic case, a very few papers can be found in literature devoted to the stress analysis in a particle reinforced composite with *anisotropic* phases; in these works, the simple "dilute composite" models only were considered. The probable reason is that an analysis of this problem requires more complicated math to be developed and applied. The most work done up to date in this area are based on using the Green's functions (point body force solution) for an infinite solid. So, Mura (1982) has derived the Eshelby's type solution for a single inclusion in an anisotropic medium. This work does not provide, however, the explicit analytic expressions for the internal stress distribution similar to those obtained by Eshelby in the isotropic case. In the particular but practically important case of transversely isotropic elastic properties, Pan and Chou (1976) have been found analytical expressions for the Green's functions and their derivatives. Based on their findings, Withers (1989) has applied the Eshelby's method to calculate the elastic field about an ellipsoidal inclusion embedded within a transversely isotropic matrix of the same elastic constants. In the Willis' (1975) work, two interacting spherical voids in an anisotropic elastic solid were considered and the problem was formulated in terms of integral equation for the "transformation stress" in equivalent homogeneous inclusion. Using the iterative perturbation technique, an explicit approximate solution has been obtained for polynomials up to second degree.

An alternate approach has been proposed by Podil'chuk (1984) (see also the recent Podil'chuk's (2001) survey paper) who considered a solid with a single inclusion subjected to the polynomial external load. His method is based on the observation that the governing equations describing steady stress in the transversely isotropic solid allow separation of variables in the properly introduced curvilinear coordinates. The resulting rigorous series solution is expressed in terms of the associated Legendre functions. It should be noted, however, that the original solution is given by Podil'chuk (1984) in a scalar form which makes it rather difficult to analyze and utilize.

In the present paper, the Podil'chuk's method is revised and expanded on the class of many-particle models of composite with transversely isotropic phases. To expose the basic technique of method, we start with the one-particle problem and obtain the exact analytical solution, written in a compact matrix-vector form, in the case of arbitrarily oriented anisotropy axes of the matrix and inclusion materials. Noteworthy, in all mentioned above works the anisotropy axes were assumed to be aligned. Then, in the subsequent sections, we apply systematically the method developed to obtain the accurate solutions for a solid containing a finite array and infinite periodic, lattice type array of inclusions. The numerical results are presented and discussed in the last section. They demonstrate an effect on stress concentration of the selected

structural parameters of composite as well as accuracy and computational efficiency of the method developed.

2. Medium with a single inclusion

In the Cartesian coordinate system $Oxyz$ with Oz axis aligned with the anisotropy axis of transversely isotropic material, the generalized Hook's law $\sigma = \mathbf{C}\cdot\varepsilon$ has a form

$$\begin{aligned}
&\sigma_x = C_{11}\varepsilon_x + C_{12}\varepsilon_y + C_{13}\varepsilon_z, \quad \tau_{xz} = 2C_{44}\varepsilon_{xz},\\
&\sigma_y = C_{12}\varepsilon_x + C_{11}\varepsilon_y + C_{13}\varepsilon_z, \quad \tau_{yz} = 2C_{44}\varepsilon_{yz},\\
&\sigma_z = C_{13}\varepsilon_x + C_{13}\varepsilon_y + C_{33}\varepsilon_z, \quad \tau_{xy} = (C_{11}-C_{12})\varepsilon_{xy}.
\end{aligned} \tag{1}$$

Here, two-indices notation $C_{ij} = C_{iijj}$ is adopted. The components of stress tensor σ satisfy the equilibrium equations $\nabla\cdot\sigma = 0$ and the small elastic strain tensor ε is related to the displacement vector $\mathbf{u}$ by $\varepsilon = \frac{1}{2}[\nabla\mathbf{u} + (\nabla\mathbf{u})^{\mathrm{T}}]$.

Let us consider an infinite solid with a single spherical inclusion of radius R embedded. Both the matrix and inclusion are elastic and transversely isotropic; at the interface S, the conditions of perfect mechanical contact

$$(\mathbf{u}^+ - \mathbf{u}^-)|_S = 0, \quad (\mathbf{T}_\mathbf{n}(\mathbf{u}^+) - \mathbf{T}_\mathbf{n}(\mathbf{u}^-))|_S = 0, \tag{2}$$

are imposed, where $\mathbf{T}_\mathbf{n} = \sigma\cdot\mathbf{n}$ the normal traction vector and $\mathbf{n}$ is the outer normal unit vector at the surface S. Here and below, all the parameters associated with the matrix and inclusion are denoted by the superscript "$-$" and "$+$", respectively. The stress state of a medium is induced by the remote constant stress tensor $\mathbf{S}$ or strain tensor $\mathbf{E} = \mathbf{C}^{-1}\cdot\mathbf{S}$ prescribed.

We assume the anisotropy axes of both the matrix and inclusion materials to be *arbitrarily* oriented and introduce the material-related Cartesian coordinate systems $Ox^-y^-z^-$ and $Ox^+y^+z^+$ with common origin in the centre of inclusion. The point coordinates and the vector components in these coordinate systems are related by

$$x_i^+ = \Omega_{ij}x_j^-, \quad u_i^+ = \Omega_{ij}u_j^-, \tag{3}$$

where $\mathbf{\Omega}$ is the rotation matrix: $\mathbf{\Omega}^{\mathrm{T}} = \mathbf{\Omega}^{-1}$ and $\det\mathbf{\Omega} = 1$. Transformation of the complex Cartesian vectors $\mathbf{e}_i$ defined in Appendix A, uses the formula

$$\mathbf{e}_i^+ = \Omega_{ij}^*\mathbf{e}_j^-, \quad \text{where } \mathbf{\Omega}^* = \mathbf{D}^{-1}\mathbf{\Omega}\mathbf{D} \quad \text{and} \quad \mathbf{D} = \begin{pmatrix} 1 & 1 & 0\\ -i & i & 0\\ 0 & 0 & 1\end{pmatrix}. \tag{4}$$

The disturbance field produced by the inclusion is vanishing at infinity and, for the external load prescribed, $\mathbf{u}^- \to \mathbf{E}\cdot\mathbf{r}$ as $|\,\mathbf{r}\,| \to \infty$. We decompose the displacement vector in the matrix domain into a sum of regular part, or far field, for a homogeneous space $\mathbf{U}_0 = \mathbf{E}\cdot\mathbf{r}$ and singular disturbance, or near field $\mathbf{U}_1$, produced by the inhomogeneity. The regular part $\mathbf{U}_0$ satisfies the equilibrium equations identically; the disturbance field $\mathbf{U}_1$ vanishes at infinity and, therefore, its series expansion contains the singular solutions $\mathbf{F}_{ts}^{(j)}$ of the governing equations (see Appendix A) only. Thus, we have

$$\mathbf{u}^- = \mathbf{U}_0 + \mathbf{U}_1 = \mathbf{E}\cdot\mathbf{r}^- + \sum_{j=1}^{3}\sum_{t=0}^{\infty}\sum_{|s|\leqslant t+1} A_{ts}^{(j)}\mathbf{F}_{ts}^{(j)}(\mathbf{r}^-). \tag{5}$$

On the contrary, the displacement field within the inclusion $\mathbf{u}^+$ has no singularity and thus can be expanded into a series over the regular solutions $\mathbf{f}_{ts}^{(j)}$ (A.11):

$$\mathbf{u}^{+}=\sum_{j=1}^{3}\sum_{t=0}^{\infty}\sum_{|s|\leqslant t+1}D_{ts}^{(j)}\mathbf{f}_{ts}^{(j)}(\mathbf{r}^{+}), \tag{6}$$

where $D_{ts}^{(j)}$ as well as $A_{ts}^{(j)}$ in (5) are the expansion coefficients to be determined from the contact conditions (2).

Expression (6) is written already in the spheroidal coordinates and the similar expansion of the regular part $\mathbf{U}_0$ follows from the formulae (A.12). After some algebra, we get

$$\mathbf{E}\cdot\mathbf{r}^{-}=\sum_{j=1}^{3}\sum_{t=0}^{\infty}\sum_{|s|\leqslant t+1}e_{ts}^{(j)}\mathbf{f}_{ts}^{(j)}(\mathbf{r}^{-}), \tag{7}$$

where

$$\begin{aligned}
e_{10}^{(1)}&=\frac{d_1^{-}v_1^{-}}{k_1^{-}v_2^{-}-k_2^{-}v_1^{-}}[E_{33}v_2^{-}+k_2^{-}(E_{11}+E_{22})],\\
e_{11}^{(1)}&=-\overline{e_{1,-1}^{(1)}}=\frac{d_1^{-}\sqrt{v_1^{-}}}{k_1^{-}}(E_{13}-\mathrm{i}E_{23}),\\
e_{12}^{(1)}&=\overline{e_{1,-2}^{(1)}}=(E_{11}-E_{22}-2\mathrm{i}E_{12}),\\
e_{10}^{(2)}&=-\frac{v_2^{-}d_2^{-}}{k_1^{-}v_2^{-}-k_2^{-}v_1^{-}}[E_{33}v_1^{-}+k_1^{-}(E_{11}+E_{22})],\\
e_{11}^{(3)}&=\overline{e_{1,-1}^{(3)}}=\frac{\sqrt{v_3^{-}}d_3^{-}}{k_1^{-}}(1-k_1^{-})(E_{13}-\mathrm{i}E_{23}),
\end{aligned} \tag{8}$$

all other coefficients $e_{ts}^{(i)}$ are equal to zero. For definiteness sake, we assume here and below $v_1\neq v_2$; in the case of equal roots v_1 and v_2 of Eq. (A.3), one has to use $\mathbf{f}_{ts}^{(2)}$ and $\mathbf{F}_{ts}^{(2)}$ in the form (A.16) rather than (A.11) in (5)–(7) and all the subsequent formulae.

To solve for the expansion coefficients, we note first that the functions $\mathbf{F}_{0s}^{(i)}$ are, in fact, the fundamental solutions representing action of the point body forces in an infinite solid. Because no body forces is suggested in the problem statement, we get immediately $A_{0s}^{(i)}\equiv 0$. The remaining coefficients $A_{ts}^{(i)}$ and $D_{ts}^{(i)}$ will be determined from the interface boundary conditions (2). To obtain a resolving set of equations for the unknowns $A_{ts}^{(i)}$ and $D_{ts}^{(i)}$ we make use the representation (A.13) of the functions $\mathbf{f}_{ts}^{(i)}$ and $\mathbf{F}_{ts}^{(i)}$ on the surface $r=R$, rewritten in the compact form as

$$\mathbf{F}_{ts}^{(i)}\,|_S=\sum_{j=1}^{3}UG_{ts}^{ji}\chi_t^{s_j}\mathbf{e}_j,\quad \mathbf{f}_{ts}^{(i)}\,|_S=\sum_{j=1}^{3}UM_{ts}^{ji}\chi_t^{s_j}\mathbf{e}_j, \tag{9}$$

where

$$\begin{aligned}
\mathbf{UG}_{ts}=\{UG_{ts}^{ij}\}&=\begin{pmatrix} Q_t^{s-1}(\xi_{10}) & Q_t^{s-1}(\xi_{20}) & Q_t^{s-1}(\xi_{30})\\ -Q_t^{s+1}(\xi_{10}) & -Q_t^{s+1}(\xi_{20}) & Q_t^{s+1}(\xi_{30})\\ \dfrac{k_1}{\sqrt{v_1}}Q_t^{s}(\xi_{10}) & \dfrac{k_2}{\sqrt{v_2}}Q_t^{s}(\xi_{20}) & 0\end{pmatrix},\\
\mathbf{UM}_{ts}=\{UM_{ts}^{ij}\}&=\begin{pmatrix} P_t^{s-1}(\xi_{10}) & P_t^{s-1}(\xi_{20}) & P_t^{s-1}(\xi_{30})\\ -P_t^{s+1}(\xi_{10}) & -P_t^{s+1}(\xi_{20}) & P_t^{s+1}(\xi_{30})\\ \dfrac{k_1}{\sqrt{v_1}}P_t^{s}(\xi_{10}) & \dfrac{k_2}{\sqrt{v_2}}P_t^{s}(\xi_{20}) & 0\end{pmatrix}
\end{aligned} \tag{10}$$

and $s_1=s-1$, $s_2=s+1$ and $s_3=s$. In these notations,

$$\mathbf{u}^- = \sum_{j=1}^{3}\sum_{t=0}^{\infty}\sum_{|l|\leqslant t+1}\left[\sum_{\alpha=1}^{3} UG_{tl}^{j\alpha-}A_{tl}^{(\alpha)} + UM_{tl}^{j\alpha-}e_{tl}^{(\alpha)}\right]\chi_t^{l_j}(\theta^-,\varphi^-)\mathbf{e}_j^- \tag{11}$$

and

$$\mathbf{u}^+ = \sum_{i=1}^{3}\sum_{t=0}^{\infty}\sum_{|s|\leqslant t+1}\left[\sum_{\alpha=1}^{3} UM_{ts}^{i\alpha+}D_{ts}^{(\alpha)}\right]\chi_t^{s_i}(\theta^+,\varphi^+)\mathbf{e}_i^+. \tag{12}$$

Note that $\mathbf{u}^-$ (11) and $\mathbf{u}^+$ (12) are still written in the different coordinate systems. Therefore, before substituting them into (2), $\mathbf{u}^+$ has to be expressed in terms of the variables θ^-, φ^- and vectors $\mathbf{e}_j^-$. For this purpose, we apply the Bateman's transformation formula of the surface spherical harmonics due to rotation of coordinate basis (Bateman and Erdelyi, 1953):

$$\chi_t^s(\theta^+,\varphi^+) = \sum_{|l|\leqslant t}\frac{(t+l)!}{(t+s)!}S_{2t}^{t-s,t-l}(\mathbf{w})\chi_t^l(\theta^-,\varphi^-), \tag{13}$$

where S_{2t}^{sl} are the spherical harmonics in four-dimensional space and $\mathbf{w}$ is the vector of Euler's parameters related to the rotation matrix $\boldsymbol{\Omega}$ by

$$\boldsymbol{\Omega} = \begin{pmatrix} w_2^2 - w_1^2 - w_3^2 + w_4^2 & 2(w_2w_3 - w_1w_4) & 2(w_1w_2 + w_3w_4) \\ 2(w_2w_3 + w_1w_4) & w_3^2 - w_1^2 - w_2^2 + w_4^2 & 2(w_1w_3 - w_2w_4) \\ 2(w_1w_2 - w_3w_4) & 2(w_1w_3 - w_2w_4) & w_1^2 - w_2^2 - w_3^2 + w_4^2 \end{pmatrix}. \tag{14}$$

Applying (13) and (4) to (12) gives

$$\mathbf{u}^+ = \sum_{j=1}^{3}\sum_{t=0}^{\infty}\sum_{|l|\leqslant t+1}\left[\sum_{i=1}^{3}\Omega_{ij}^*\sum_{|s|\leqslant t+1}\frac{(t+l_j)!}{(t+s_i)!}S_{2t}^{t-s_i,t-l_j}(\mathbf{w})\times\sum_{\alpha=1}^{3}UM_{ts}^{i\alpha+}D_{ts}^{(\alpha)}\right]\chi_t^{l_j}(\theta^-,\varphi^-)\mathbf{e}_i^-. \tag{15}$$

Now, we substitute $\mathbf{u}^-$ (11) and transformed expression of $\mathbf{u}^+$ (15) into the first of conditions (2) and make use of the orthogonality property of spherical harmonics χ_t^s on the surface S to decompose vectorial functional equality $\mathbf{u}^+ = \mathbf{u}^-$ into a set of linear algebraic equations. It can be written in the compact matrix-vector form as

$$\mathbf{UG}_{tl}^-\cdot\mathbf{A}_{tl} + \mathbf{UM}_{tl}^-\cdot\mathbf{e}_{tl} = \sum_{|s|\leqslant t+1}\mathbf{UM}_{tsl}^*\cdot\mathbf{D}_{ts}, \quad t = 0,1,2,\ldots,\ |\,l\,| \leqslant t+1, \tag{16}$$

where

$$\begin{aligned} &\mathbf{UM}_{tsl}^* = \mathbf{W}_{tsl}\mathbf{UM}_{ts}^+, \quad W_{tsl}^{ji} = \Omega_{ij}^*\frac{(t+l_j)!}{(t+s_i)!}S_{2t}^{t-s_i,t-l_j}(\mathbf{w}), \\ &\mathbf{A}_{tl} = (A_{tl}^{(1)},A_{tl}^{(2)},A_{tl}^{(3)})^{\mathrm{T}}, \quad \mathbf{D}_{tl} = (D_{tl}^{(1)},D_{tl}^{(2)},D_{tl}^{(3)})^{\mathrm{T}} \quad \text{and} \\ &\mathbf{e}_{tl} = (e_{tl}^{(1)},e_{tl}^{(2)},e_{tl}^{(3)})^{\mathrm{T}}. \end{aligned} \tag{17}$$

Obtaining the second set of equations follows the same procedure where, instead of (A.13), the representation (A.14) of the normal traction vectors $\mathbf{T}_{\mathbf{n}}(\mathbf{f}_{ts}^{(j)})$ and $\mathbf{T}_{\mathbf{n}}(\mathbf{f}_{ts}^{(j)})$ on the surface $r = R$ has to be utilized. After transformations, we obtain

$$\mathbf{TG}_{tl}^-\cdot\mathbf{A}_{tl} + \mathbf{TM}_{tl}^-\cdot\mathbf{e}_{tl} = \sum_{|s|\leqslant t+1}\mathbf{TM}_{tsl}^*\cdot\mathbf{D}_{ts}, \tag{18}$$

where $\mathbf{TM}_{tsl}^* = \mathbf{W}_{tsl}\mathbf{TM}_{ts}^+$. Form of the matrices $\mathbf{TG}_{tl}$ and $\mathbf{TM}_{tl}$ is clear from (A.14). Eqs. (16) and (18) together form a complete set of linear equations from where $A_{ts}^{(i)}$ and $D_{ts}^{(i)}$ can be determined. To reduce

dimension of the linear system to be solved, one can eliminate $\mathbf{A}_{tl}$ to get the set of equations involving the unknowns $\mathbf{D}_{ts}$ only:

$$\sum_{|s|\leqslant t+1}[(\mathbf{TG}_{tl}^{-})^{-1}\mathbf{TM}_{tsl}^{*}-(\mathbf{UG}_{tl}^{-})^{-1}\mathbf{UM}_{tsl}^{*}]\cdot\mathbf{D}_{ts}=[(\mathbf{TG}_{tl}^{-})^{-1}\mathbf{TM}_{tl}^{-}-(\mathbf{UG}_{tl}^{-})^{-1}\mathbf{UM}_{ll}^{-}]\cdot\mathbf{e}_{ts},$$
$$t=0,1,2,\ldots,\ |\ l\ |\ \leqslant t+1. \tag{19}$$

After we have solved (19) for $\mathbf{D}_{ts}$, either (16) of (18) can be applied to determine $\mathbf{A}_{tl}$ and, thus, accomplish solution of the problem.

An attempt to solve the linear system (19) discovers, however, that its determinant is equal to zero. The reason is that, at a given t, some of the functions $\mathbf{f}_{ts}^{(i)}$ at $|\ s\ |\ \geqslant t$ are linearly dependent: e.g., $\mathbf{f}_{t,t+1}^{(1)}\sim\mathbf{f}_{t,t+1}^{(2)}$ and $\mathbf{f}_{t,t+1}^{(2)}\sim\mathbf{f}_{t,t+1}^{(3)}$. Really, we have $3(2t+3)$ vectorial solutions of order t introduced whereas the number of independent functions is equal to $3(2t+1)$ (remind, the Cartesian components of $\mathbf{f}_{ts}^{(i)}$ are the polynomials of order t (A.11) and $f_t^s\equiv 0$ for $|\ s\ |>t$). Due to the same reason, not all the $e_{1s}^{(j)}$ are represented in (8). Adding six additional constraints $D_{t,\pm t}^{(2)}=0, D_{t,\pm(t+1)}^{(2)}=0$ and $D_{t,\pm(t+1)}^{(3)}=0$ to (19) gives, finally, a well-posed set of linear equations possessing an unique solution.

It is also straightforward to show (Podil'chuk, 1984) that, although the functions $\mathbf{F}_{t,\pm(t+1)}^{(j)}$ (six in total for a given t) are discontinuous at $z=0$, the resulting displacement $\mathbf{u}^{-}$ (5) is continuous and differentiable provided we have the expansion coefficients $A_{ts}^{(i)}$ determined from (16) or (18). In fact, we have there exactly 6 equations (with $|l|=t+1$) to determine $A_{t,\pm(t+1)}^{(i)}$ in a way that the breaks in each separate function $\mathbf{F}_{t,\pm(t+1)}^{(j)}$ cancel each other. Alternatively, one can utilize these 6 equations to introduce, from the very beginning, a set of $3(2t+1)$ singular *continuous* solutions of order t, being, naturally, the linear combinations of $\mathbf{F}_{ts}^{(j)}$. This approach, however, is disadvantageous in that the introduced in such a way singular partial solutions have rather complicated structure which results, in turn, in much more involved theory as compared with that presented above.

And, to complete this section, we note the following. First, because $\mathbf{e}_{ts}\equiv 0$ for $t\neq 1$ in (8), only $A_{1s}^{(i)}$ and $D_{1s}^{(i)}$ are non-zero in the solution obtained. Moreover, in the case of aligned anisotropy axes $\mathbf{\Omega}=\mathbf{I}$ and $W_{tsl}^{ji}=\delta_{ij}\delta_{sl}$ and the system (19) breaks down onto 5 separate sets of each value of index s to give a compact form of the Podil'chuk's (1984) solution. The solution we have found for the simple loading type is of finite form and exact. However, all the theory developed is valid and the solution remains exact for the arbitrary polynomial external load. In this case, the series expansions (6) and (8) contains the higher $(t>1)$ harmonics as well. In the subsequent sections, this feature will be used to derive accurate, asymptotically exact solutions of the many-particle problems.

3. Finite array of inclusions

Let us consider now an unbounded domain containing N non-touching spherical particles of radius R_q with the centres located in the points O_q, $q=1,2,\ldots,N$ and the elastic stiffness tensors $\mathbf{C}_q^{+}$. We introduce the local material-related coordinate systems $Ox_q^{+}y_q^{+}z_q^{+}$ which origin and orientation with respect to the global Cartesian coordinate system $Ox^{-}y^{-}z^{-}$ is defined by the vector $\mathbf{R}_q$ and the rotation matrix $\mathbf{\Omega}_q$ (Fig. 1).

The matrix–inclusion interface boundary conditions are

$$(\mathbf{u}_q^{+}-\mathbf{u}^{-})\ |_{S_q}=0,\quad(\mathbf{T}_{\mathbf{n}}(\mathbf{u}_q^{+})-\mathbf{T}_{\mathbf{n}}(\mathbf{u}^{-}))\ |_{S_q}=0,\quad q=1,2,\ldots,N, \tag{20}$$

the stress state of the inhomogeneous medium is governed, as before, by the constant load applied at infinity.

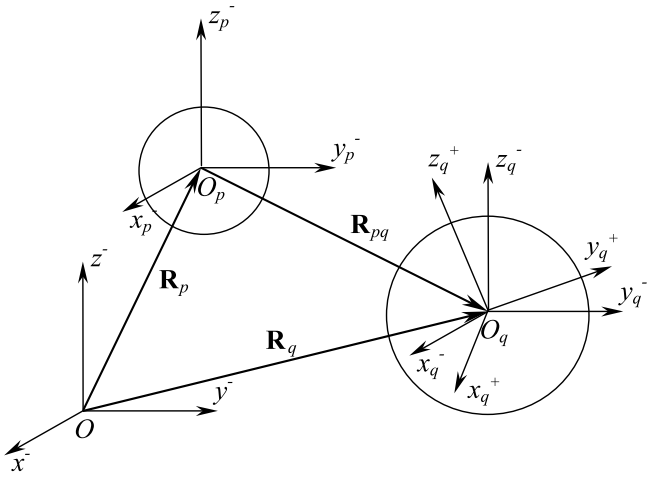

Fig. 1. Geometry of the many-particle model.

In (20), $\mathbf{u}_q^+$ is the displacement vector in the volume of qth inclusion which, by analogy with (6) can be written as

$$\mathbf{u}_q^+ = \sum_{j=1}^{3} \sum_{t=0}^{\infty} \sum_{|s| \leqslant t+1} D_{ts}^{(q)(j)} \mathbf{f}_{ts}^{(j)}(\mathbf{r}_q^+). \tag{21}$$

To construct the solution in the multiply-connected matrix domain, we shall follow the procedure described by Kushch (1996). According to the generalized superposition principle, the displacement vector $\mathbf{u}^-$ can be written as a sum of linear far field and the disturbance fields induced by each separate inclusion:

$$\mathbf{u}^- = E \cdot \mathbf{r}^- + \sum_{p=1}^{N} \mathbf{U}_p(\mathbf{r}_p^-), \quad \mathbf{r}_p^- = \mathbf{r}^- - \mathbf{R}_p. \tag{22}$$

By analogy with (5), each singular term $\mathbf{U}_p$ allows the series expansion in the form

$$\mathbf{U}_p(\mathbf{r}_p^-) = \sum_{j=1}^{3} \sum_{t=0}^{\infty} \sum_{|s| \leqslant t+1} A_{ts}^{(p)(j)} \mathbf{F}_{ts}^{(j)}(\mathbf{r}_p^-), \tag{23}$$

where $A_{ts}^{(p)(j)}$ as well as $D_{ts}^{(q)(j)}$ in (21) are the series expansion coefficients to be found from the boundary conditions (20). It is evident that for $\mathbf{u}^-$ taken in the form (21) and (22), the condition $\mathbf{u}^- \to \mathbf{E} \cdot \mathbf{r}$ at infinity is satisfied.

Note that the separate terms of the sum in (21) are written in the different coordinate systems. To enable application the procedure described in the previous section, we need first to express $\mathbf{u}^-$ in the variables of the local, say qth, coordinate system. Such a transform is based on using the re-expansion formulae for the singular vectorial solutions $\mathbf{F}_{ts}^{(j)}$ due to translation of the coordinate system origin:

$$\mathbf{F}_{ts}^{(j)}(\mathbf{r}_p^-) = \sum_{k=0}^{\infty} \sum_{|l| \leqslant k+1} \eta_{tk}^{s-l}(\mathbf{R}_{pq}, d_{pj}^-, d_{qj}^-) \mathbf{f}_{kl}^{(j)}(\mathbf{r}_q^-), \quad t = 0, 1, 2, \ldots, \ |s| \leqslant t+1. \tag{24}$$

The formulae (24) follow directly from the corresponding result for the scalar harmonic functions F_t^s (Kushch, 1997a)

$$F_t^s(\mathbf{r}_p, d_p) = \sum_{k=0}^{\infty} \sum_{|l| \leqslant k} \eta_{tk}^{s-l}(\mathbf{R}_{pq}, d_p, d_q) f_k^l(\mathbf{r}_q, d_q), \quad \mathbf{R}_{pq} = \mathbf{R}_p - \mathbf{R}_q \tag{25}$$

and provide a series expansion of the field with a singularity in the point O_p in a vicinity of the point O_q where the field is regular. Expectably, the series in (24) contains the regular solutions $\mathbf{f}_{kl}^{(j)}$ only. For the explicit form of the re-expansion coefficients η_{tk}^{s-l}, details of derivation and convergence analysis, see also Kushch and Sangani (2000).

It is important to note that the functions F_t^{t+k} (A.9) are introduced in such a way that the formula (25) remains valid for the extended set of singular spheroidal harmonics F_t^s including those defined by (A.9) for $|s| \leqslant t+2$. We apply (24) to all the sum terms in (22) but that one with $p = q$ which is written initially in the variables of this local coordinate system. After some algebra, we find

$$\mathbf{u}^-(\mathbf{r}_q^-) = \sum_{j=1}^{3} \sum_{t=0}^{\infty} \sum_{|s| \leqslant t+1} [A_{ts}^{(q)(j)} \mathbf{F}_{ts}^{(j)}(\mathbf{r}_q^-) + (a_{ts}^{(q)(j)} + e_{ts}^{(q)(j)}) \mathbf{f}_{ts}^{(j)}(\mathbf{r}^-)], \tag{26}$$

where

$$a_{ts}^{(q)(j)} = \sum_{k=0}^{\infty} \sum_{|l| \leqslant k+1} \sum_{\substack{p=1 \\ p \neq q}}^{N} \eta_{kt}^{l-s}(\mathbf{R}_{pq}, d_{pj}^-, d_{qj}^-) A_{kl}^{(p)(j)} \tag{27}$$

and $e_{ts}^{(q)(j)}$ are the expansion coefficients of the linear part of (22) given by the formula (8), with replace d_j^- to $d_{qj}^- = R_q / \xi_{j0}^-$.

After the local expansion of $\mathbf{u}^-$ in the vicinity of the point O_q is found, the remaining part of solving procedure follows the way described in Section 2. In fact, by using the re-expansion formulae (24) we have reduced the primary many-particle problem to a coupled set of N "a medium with one inclusion in the inhomogeneous external field" problems. The resulting *infinite* set of linear algebraic equations are

$$\begin{aligned}
&\mathbf{UG}_{tl}^{(q)-} \cdot \mathbf{A}_{tl}^{(q)} + \mathbf{UM}_{tl}^{(q)-} \cdot (\mathbf{a}_{tl}^{(q)} + \mathbf{e}_{tl}^{(q)}) = \sum_{|s| \leqslant t+1} \mathbf{UM}_{tsl}^{(q)*} \cdot \mathbf{D}_{ts}^{(q)}, \\
&\mathbf{TG}_{tl}^{(q)-} \cdot \mathbf{A}_{tl}^{(q)} + \mathbf{TM}_{tl}^{(q)-} \cdot (\mathbf{a}_{tl}^{(q)} + \mathbf{e}_{tl}^{(q)}) = \sum_{|s| \leqslant t+1} \mathbf{TM}_{tsl}^{(q)*} \cdot \mathbf{D}_{ts}^{(q)}, \\
&q = 1, 2, \ldots, N, \;\; t = 0, 1, 2, \ldots, \;\; |\, l \,| \leqslant t+1,
\end{aligned} \tag{28}$$

where $\mathbf{a}_{tl}^{(q)} = (a_{ts}^{(q)(j)}, a_{ts}^{(q)(j)}, a_{ts}^{(q)(j)})^{\mathrm{T}}$ and $a_{ts}^{(q)(j)}$ are given by (27). Its approximate solution can be obtained, say, by the truncation method, when the unknowns and equations with $t \leqslant t_{\max}$ only are retained in (28). The

Table 1
Convergence of the matrix stress σ_z^-/S_{33} with $t_{\max}$ increased

$t_{\max}$	$X_{12} = 2.1R$		$X_{12} = 2.2R$		$X_{12} = 2.5R$	
	$\varphi = 0$	$\varphi = \pi$	$\varphi = 0$	$\varphi = \pi$	$\varphi = 0$	$\varphi = \pi$
1	3.500	3.500	3.458	3.458	3.393	3.393
3	4.079	3.518	3.821	3.447	3.510	3.370
5	4.593	3.485	4.074	3.417	3.554	3.359
7	4.944	3.447	4.215	3.395	3.570	3.356
9	5.154	3.419	4.283	3.382	3.576	3.354
11	5.271	3.401	4.313	3.375	3.579	3.354
13	5.334	3.392	4.325	3.373	3.579	3.354
15	5.368	3.386	4.330	3.371	3.579	3.354
17	5.387	3.384	4.331	3.371	3.579	3.354

solution is convergent for $t_{\max} \to \infty$ provided that the non-touching conditions $\|\mathbf{R}_{pq}\| > R_p + R_q$ are satisfied for each pair of inclusions. Thus, we can solve (28) for $\mathbf{A}_{tl}^{(q)}$ and $\mathbf{D}_{ts}^{(q)}$ with any desirable accuracy by taking $t_{\max}$ sufficiently large. It is seen form Table 1 in Section 5 that the convergence rate is sufficiently high for a whole range of the problem parameters excluding only the nearly-touching inclusions. Analysis of this extreme case is, however, beyond the scope of this paper.

4. Spatially periodic array of inclusions

The third well-known model of composite we consider here is an unbounded medium containing a spatially periodic array of inclusions. For the simplicity's sake, we assume all the particles to be identical and located in the nodes of simple cubic lattice with the period a. The elementary periodicity cell of such a structure is the cube with side a containing one inclusion embedded. The matrix–inclusion interface conditions are given by (2) whereas the loading parameter $\mathbf{E}$ has now a meaning of the macroscopic strain tensor.

$$\mathbf{E} = \langle \varepsilon \rangle = \frac{1}{V} \int_V \varepsilon \, \mathrm{d}V, \tag{29}$$

V being a volume of the periodicity cell. Alternatively, the governing parameter can be taken in the form of macroscopic stress tensor, $\mathbf{S} = \langle \sigma \rangle = \frac{1}{V} \int_V \sigma \, \mathrm{d}V$. Here, we consider macroscopically homogeneous stress state of composite assuming both the $\mathbf{E}$ and $\mathbf{S}$ to be constant.

This model may be thought, in particular, as a limiting case of the ordered finite array in which the number of particles N becomes infinitely large. Likewise, the appropriate form of solution for this model is given by (22) where $N \to \infty$. Taking the periodicity of solution pre-determined by the periodicity of structure into account we find that $\mathbf{A}_{tl}^{(q)}$ must have the same value for any q. Then, omitting this index in (22) and (23), we write a formal solution as

$$\mathbf{u}^- = \mathbf{E} \cdot \mathbf{r}^- + \sum_{j=1}^{3} \sum_{t=0}^{\infty} \sum_{|s| \leqslant t+1} A_{ts}^{(j)} \widehat{\mathbf{F}}_{ts}^{(j)}(\mathbf{r}^-), \tag{30}$$

where

$$\widehat{\mathbf{F}}_{ts}^{(j)}(\mathbf{r}) = \sum_p \mathbf{F}_{ts}^{(j)}(\mathbf{r} - \mathbf{R}_p) \tag{31}$$

and summation is made over all the lattice nodes. Provided that $\widehat{\mathbf{F}}_{ts}^{(j)}$ are the triply periodic functions, the displacement vector (30) comply the condition (29). The method of summation and detailed convergence analysis of the triple series (31) is given elsewhere (Kushch and Sevostianov, 2003). Here, we apply formally the technique developed in Section 3 for a finite array of inclusions to (30) and obtain the resolving set of equations in the form (28), with the superscript (q) omitted, and

$$a_{ts}^{(j)} = \sum_{k=0}^{\infty} \sum_{|l| \leqslant k+1} \widehat{\eta}_{kt}^{(l-s)}(d_j^-) A_{kl}^{(j)}, \tag{32}$$

where the matrix coefficients are the triple infinite (lattice) sums

$$\widehat{\eta}_{kt}^{(l-s)}(d) = \sum_{p \neq 0} \eta_{kt}^{(l-s)}(\mathbf{R}_p, d, d). \tag{33}$$

Now, we recognize that (33) are exactly the sums appearing in the conductivity problem solution for a composite with transversely isotropic phases obtained by Kushch (1997a). There, convergence of the series

(33) was discussed and the fast summation technique has been developed. The only difference here is the extended variation range of indices s and l in (33). Fortunately, these series converge, conditionally at least, for all values of indices $|s| \leqslant t+1$ and $|l| \leqslant k+1$ provided that the non-touching condition $a > 2R$ is satisfied.

5. Numerical results

In this Section, we give a few numerical examples demonstrating computational efficiency and accuracy of the method developed and showing, at the same time, how the structural parameters and phase anisotropy influence the microstress concentration in a composite. Noteworthy, numerical algorithm of the method is rather simple and consists in calculating the matrix coefficients of linear system followed by solving it with the standard linear solver routine. The typical number of unknowns retained in the resolving set of equations varies from single-digit numbers to a few hundreds depending on complexity of the problem being considered. This is a very moderate number in comparison with the tens and hundreds of thousand equations in the 3D finite element analysis of similar problems which proves the above algorithm to be highly efficient form the computational standpoint.

We begin our numerical analysis from the single inclusion problem considered in Section 2. Even this simplest model has a number of parameters, they are five components of the matrix $\mathbf{C}^-$, five components of the matrix $\mathbf{C}^+$, three components of the rotation matrix $\mathbf{\Omega}$ and the particle radius R. In practical applications, it is often more convenient to use the so-called "technical" elastic constants, namely the Young moduli E_i, the shear moduli G_{ij} and the Poisson's ratios ν_{ij} rather than the components C_{ij} of the elastic stiffness tensor. In the case of transversely isotropic body, they are related to C_{ij} by

$$\begin{aligned} &G_{12} = \tfrac{1}{2}(C_{11} - C_{12}), \quad G_{23} = G_{13} = C_{44}, \\ &E_1 = E_2 = 2\left(\frac{1}{C_{11} - C_{12}} + \frac{C_{33}}{\Delta}\right)^{-1}, \quad E_3 = \frac{\Delta}{(C_{11} + C_{12})}, \\ &\nu_{13} = \nu_{23} = C_{13}/(C_{11} + C_{12}), \quad \nu_{12} = \frac{E_1}{2}\left(\frac{1}{C_{11} - C_{12}} - \frac{C_{33}}{\Delta}\right), \end{aligned} \tag{34}$$

where $\Delta = (C_{11} + C_{12})C_{33} - 2(C_{13})^2$ and only five of these constants are independent. The elastic moduli introduced by (34) are more physically tractable and so will be taken as the input parameters in our numerical analysis. In particular, either E_3/E_1 or $G_{13}/G_{12} = 2C_{44}/(C_{11} - C_{12})$ can be chosen as a measure of anisotropy degree.

A complete parametric study of the problems considered above is not a subject of the present paper. Although in all the above solutions no restrictions (but the particle-to-particle non-touching condition) were imposed on the structure, phase properties and loading type, in the subsequent numerical study we shall keep most of the parameters fixed and present the numerical data giving a general idea how the selected structure parameters, namely distance between the particles, their relative position, misalignment of the phase materials anisotropy axes and anisotropy degree affect the stress field around inhomogeneities. First, uniaxial tension is the only external loading type being considered here. Next, we restrict rotation of inclusion to the xz-plane: in this case, the only variable Euler's parameter is the angle β between the Oz^- and Oz^+ axes. To minimize number of the independent elastic constants, we put $\nu_{12}^+ = \nu_{12}^- = 0.3$, $\nu_{13}^+ = \nu_{13}^- = 0.3$, $G_{13}^- = 1$ and $E_1 = 2.6$. Two variable material-related parameters are the matrix anisotropy degree $A = E_3^-/E_1^-$ and the inclusion-to-matrix stiffness ratio, λ. Thus, we have $E_3^- = AE_1^-$, $G_{13}^+ = \lambda G_{13}^-$, $E_1^+ = \lambda E_1^-$ and $E_3^+ = \lambda E_3^-$. Two extreme cases here are $\lambda = 0$ and ∞, corresponding to the cavity and rigid particle. For the elastic inclusion $E_3^+/E_1^+ = A$; i.e., we assume the inclusion's anisotropy degree to be equal to that of the matrix material.

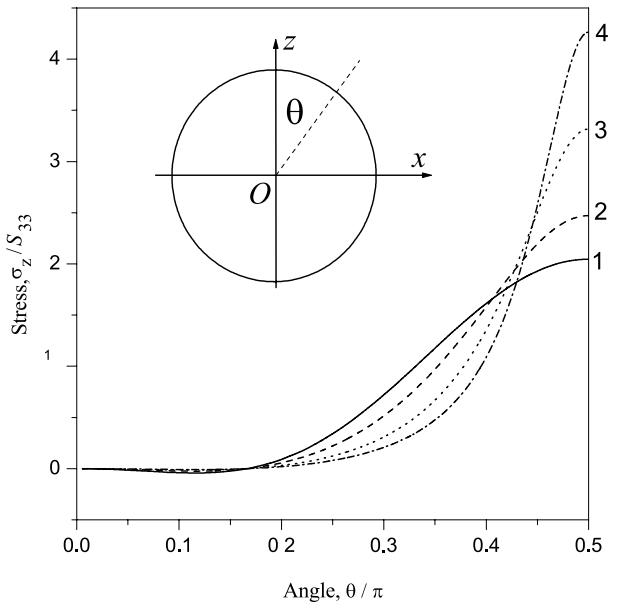

Fig. 2. Stress σ_z^- variation along the cavity surface: (line 1) $A = 1$; (line 2) $A = 2$; (line 3) $A = 5$; (line 4) $A = 10$.

First, we consider a medium with a single spherical cavity, $\lambda = 0$. In Fig. 2, the normalized stress $\sigma_z^-(\theta)/S_{33}$ variation along the cavity surface meridian $R = 1$, $0 \leqslant \theta \leqslant \pi/2$, $\varphi = 0$ calculated for the anisotropy parameter A equal to 1 (isotropic matrix), 2, 5 and 10 is shown by the lines 1–4, respectively. Expectably, the maximum stress σ_z^- is located at the cavity's equator and grows up more than two times as A

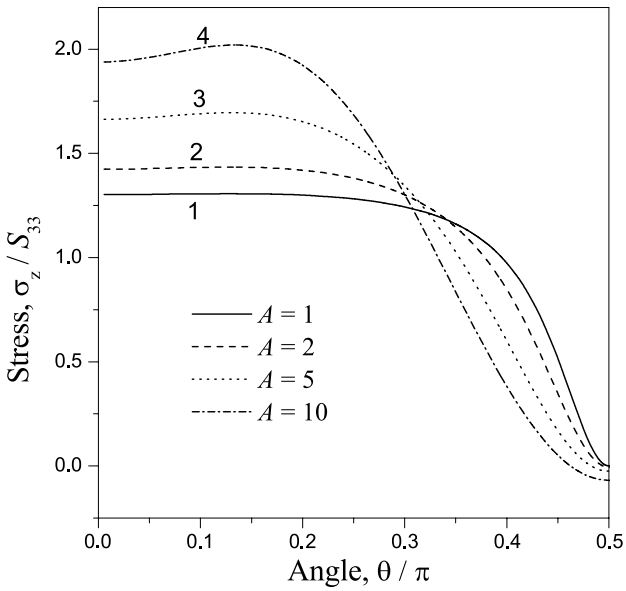

Fig. 3. Stress σ_z^- variation along the matrix–rigid particle interface: (line 1) $A = 1$; (line 2) $A = 2$; (line 3) $A = 5$; (line 4) $A = 10$.

varies from 1 to 10. The similar data for a medium containing one rigid inclusion ($\lambda = \infty$) are given in Fig. 3. By contrast with the cavity case, the stress concentration at the particle-matrix interface decreases with A increased. In both Figs. 2 and 3, the line 1 represents the well-known Lame solution for an isotropic medium being a trivial limiting case of the solution obtained in Section 2.

The interesting example is a medium containing a single elastic inclusion made of the same material as the matrix does: $\mathbf{C}^+ = \mathbf{C}^-$. The matrix stress σ_z^- variation along the matrix–inclusion interface is plotted in Fig. 4. The curve 1 corresponds to the trivial case of aligned Oz^- and Oz^+ axes ($\beta = 0$) where we have a homogeneous material with no stress concentration: $\sigma_z^- \equiv S_{33}$. However, even a small misalignment of the matrix and inclusion material anisotropy axes leads to significant peak stress growth. The lines 2–4 show $\sigma_z^-(\theta)/S_{33}$ for $\beta = \pi/10$, $3\pi/20$ and $\pi/2$. In the last case, the stress concentration factor $k_{33} = \max \sigma_z^-(\theta)/S_{33}$ is equal to 2.45. The situation considered here is rather typical for the majority of polycrystalline materials with misaligned anisotropic grains. As we have shown already, orientation factor can contribute considerably to the microstructural stress and, thus, affect the material's properties. The magnitude of this stress is dependent on the material anisotropy degree A: in Fig. 5, k_{33} is plotted as a function the rotation angle β. The curves 1–3 represent $k_{33}(\beta)$ calculated for $A = 2$, 5 and 10. It is seen from these plots that the $\max k_{33}$ can be estimated roughly as $\sqrt{A}$. This observation is valid, however, for the specific material and loading type: to investigate effect of anisotropy and orientation thoroughly, much more additional work has to be done.

Now, we consider a solid containing two particles/cavities and investigate how the distance between them influences the stress field around them. We assume the inhomogeneities to be identical with the centres lying on the Ox^- axis and the anisotropy axes aligned. The additional structure parameter in this problem is a distance between the centres of inclusions, $X_{12} = \|\mathbf{R}_{12}\|$. Remind that, unlike the one-particle case, solution of this problem is an infinite series. For calculations, we retain in the theoretical solution a finite number of harmonics with $t \leqslant t_{\max}$. To estimate accuracy of the numerical results obtained, we need to learn about the convergence of the truncated solution with $t_{\max}$ increased. In Table 1, the values $\sigma_z^-(t_{\max})$ calculated in the equator points $P_1(\theta = \pi/2, \varphi = 0)$ and $P_2(\theta = \pi/2, \varphi = \pi)$ of the first cavity; $\lambda = 0$ and $A = 5$.

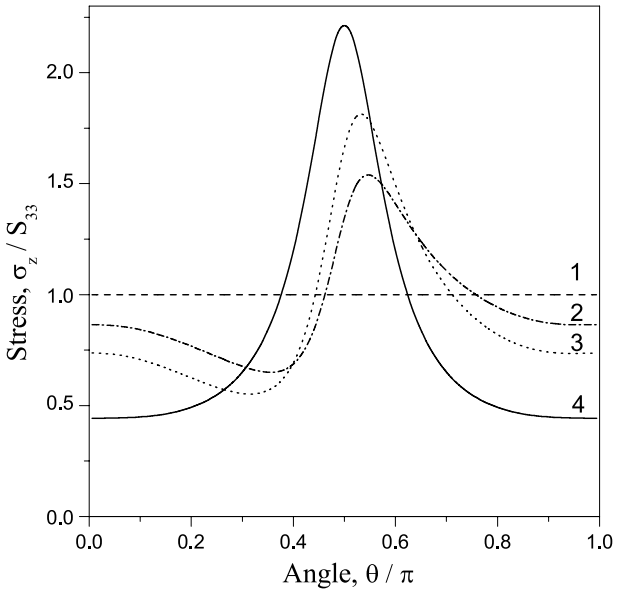

Fig. 4. Stress σ_z^- variation along the matrix–inclusion surface as a function of the angle β between the matrix and inclusion anisotropy axes: (line 1) $\beta = 0$; (line 2) $\beta = \pi/10$; (line 3) $\beta = 3\pi/20$; (line 4) $\beta = \pi/2$.

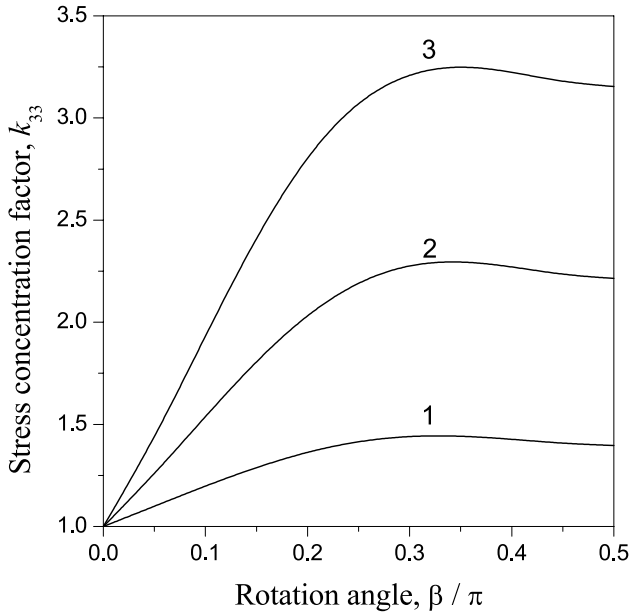

Fig. 5. Stress concentration factor k_{33} as a function of the angle β between the matrix and inclusion anisotropy axes: (line 1) $A = 2$; (line 2) $A = 5$; (line 3) $A = 10$.

The P_1 is the point nearest to the other inhomogeneity: as a result, stress in this point has a maximum whereas the convergence rate is lower than at the opposite, far side of pore. It is clearly seen from the table that the convergence rate is slowing down as the cavities approach each other: so, for $X_{12} = 2.5R$ the value $t_{\max} = 10$ provides four-digit accuracy of stress evaluation. For the nearly located cavities $X_{12} = 2.1R$, an estimated relative error of σ_z^- does not exceed 1% for $t_{\max} \geqslant 15$. Based on this analysis, the harmonics up to $t_{\max} = 15$ were retained in the subsequent computations.

The stress concentration factor k_{33} in a solid with two spherical cavities is given in Table 2 as a function of the anisotropy degree A and relative distance between the centres of cavities, X_{12}/R. In the single cavity limit ($X_{12} = \infty$), the peak σ_z^- stress values are the same as shown in Fig. 2; with X_{12} decreased, we observe considerable growth of k_{33}, which is, however, slightly slower at higher A values. For example, the ratio $k_{33}(2.1)/k_{33}(\infty)$ is equal to 1.75 for isotropic matrix and 1.55 for $A = 10$. The distance between two rigid particles has even more prominent effect on the stress concentration in the matrix. The stress concentration factor $k_{11} = \max \sigma_x^-(\theta)/S_{11}$ values due to the uniaxial tension in x-direction are given in Table 3. Here, the ratio $k_{11}(2.1)/k_{11}(\infty)$ is about 6 and, surprisingly, depends on A only marginally.

The geometry of our third model, being a simple cubic array of particles embedded in the transversely isotropic matrix can be defined either by the distance a between the neighboring particles or by the volume content c of dispersed phase $c = \frac{4}{3}\pi(R/a)$. To be consistent with previous analysis, we take the averaged

Table 2
Stress concentration factor $k_{33} = \max \sigma_z^-(\theta)/S_{33}$ in a solid with two spherical cavities

A	$X_{12}/R = \infty$	$X_{12}/R = 2.5$	$X_{12}/R = 2.3$	$X_{12}/R = 2.2$	$X_{12}/R = 2.1$
1.0	2.05	2.23	2.54	2.87	3.58
2.0	2.47	2.68	3.00	3.37	4.25
5.0	3.32	3.58	3.92	4.33	5.39
10.0	4.27	4.59	4.97	5.42	6.61

Table 3
Stress concentration factor $k_{11} = \max \sigma_x^-(\theta)/S_{11}$ in a solid with two rigid spherical inclusions

A	$X_{12}/R = \infty$	$X_{12}/R = 2.5$	$X_{12}/R = 2.3$	$X_{12}/R = 2.2$	$X_{12}/R = 2.1$
1.0	2.02	3.96	5.57	7.85	13.1
2.0	2.00	3.98	5.58	7.42	12.3
5.0	2.01	3.99	5.52	7.28	11.9
10.0	2.01	4.0	5.53	7.27	11.9

stress tensor $\mathbf{S} = \langle\sigma\rangle$ rather than $\mathbf{E} = \langle\varepsilon\rangle$ as a governing parameter of the problem. In order to simulate the macroscopic uniaxial tension of composite, components of the tensor $\mathbf{E}$ were chosen in a way that the condition $S_{ij} = \delta_{i3}\delta_{j3}$ is satisfied. The curves in Fig. 6 show the matrix stress σ_z^-/S_{33} variation along the matrix–inclusion interface in the composite with $A = 3$ and $\lambda = 100$.

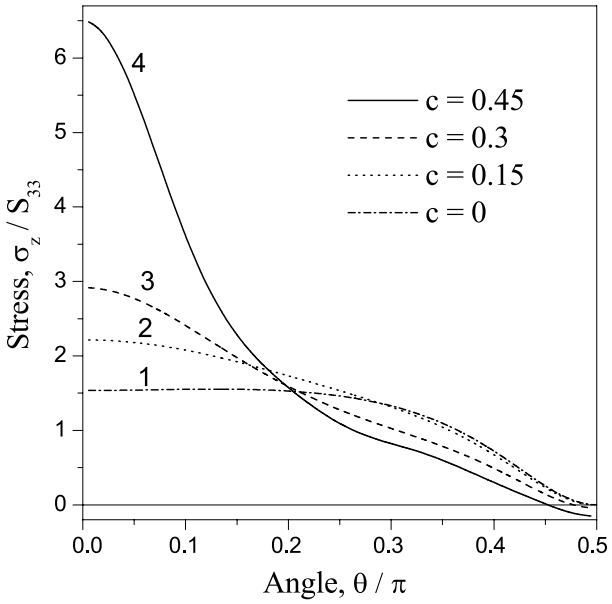

Fig. 6. Stress σ_z^- variation along the matrix–inclusion interface in the periodic composite with $A = 3$ and $\lambda = 100$: (line 1) $c = 0$; (line 2) $c = 0.15$; (line 3) $c = 0.30$; (line 4) $c = 0.45$.

Table 4
Stress concentration factor k_{33} in a composite with elastic spherical inclusions, $A = 3$

λ	$c = 0$	$c = 0.15$	$c = 0.30$	$c = 0.45$
0.1	2.38	2.50	2.94	3.07
0.5	1.48	1.55	1.66	1.83
1.0	1.0	1.0	1.0	1.0
2.0	1.22	1.42	1.49	1.58
10.0	1.48	2.00	2.45	3.76
100.0	1.55	2.21	2.92	6.47

The results obtained for the composite with a volume fraction of dispersed phase $c = 0.1$, 0.15, 0.3 and 0.45 are shown by the lines 1–4, respectively. It is seen from these plots that the maximum tensile stress σ_z^- is localized in area between the hard particles and for $c = 0.45$ is more than four times higher than that in the solid with a single inclusion. The values of stress concentration factor k_{33} as a function of c and λ are given in Table 4.

As the parametric study shows, $\partial k_{33}/\partial c$ is always positive, no matter softer or harder are the particles in comparison with the matrix material.

6. Conclusions

The accurate and efficient analytical method has been developed to study the microstress field in a particulate composite with transversely isotropic elastic phases. The essence of method is the multipole expansion technique reducing the complicated primary boundary-value problem for 3D multiple-connected domain to an ordinary set of linear algebraic equations and providing, thus, its high numerical efficiency. The method has been applied systematically to solve for stress in three basic models of particulate composite, namely a solid containing one, a finite array and an infinite spatially periodic array of spherical inclusions. The solution obtained for a single inclusion problem is finite-form and exact; for the many-particle problems, the method provides an asymptotically exact series solution. The numerical results are given demonstrating an accuracy and numerical efficiency of the method and disclosing the way and extent to which the selected structural parameters influence the stress concentration at the matrix–inclusion interface.

The method exposed above is flexible enough to be generalized in many ways. The possible next steps in developing the given approach include the detailed parametric study of the microstress concentrations and the macroscopic elastic properties of composite with transversely isotropic phases based on more realistic model of microstructure. Also, the method with minor modifications (Kushch, 1997a) can be applied to study the effect of phase anisotropy in the composites with ellipsoidal inclusions and penny-shaped cracks.

Acknowledgement

I wish to thank Dr. I. Sevostianov for attracting my attention to the problem and for the helpful discussions.

Appendix A. Partial solutions of the equilibrium equations of transversely-isotropic elastic solid

The well known fact (e.g. Podil'chuk, 1984) is that a solution of the equilibrium equations $\nabla \cdot \sigma = 0$ can be represented by means of three potential functions

$$u_x = \frac{\partial \Phi_1}{\partial x} + \frac{\partial \Phi_2}{\partial x} + \frac{\partial \Phi_3}{\partial y}, \quad u_y = \frac{\partial \Phi_1}{\partial y} + \frac{\partial \Phi_2}{\partial y} - \frac{\partial \Phi_3}{\partial x}, \quad u_z = k_1 \frac{\partial \Phi_1}{\partial z} + k_2 \frac{\partial \Phi_2}{\partial z}. \tag{A.1}$$

These functions satisfy the equation

$$\left(\frac{\partial^2}{\partial x^2} + \frac{\partial^2}{\partial y^2} + v_j \frac{\partial^2}{\partial z^2} \right) \Phi_j = 0, \quad j = 1, 2, 3, \tag{A.2}$$

where $v_3 = 2C_{44}/(C_{11} - C_{12})$ whereas v_1 and v_2 are the roots of equation

$$C_{11}C_{44}v^2 - [(C_{44})^2 - C_{11}C_{33} - (C_{13} + C_{44})^2]v + C_{33}C_{44} = 0. \tag{A.3}$$

Expressions of k_1 and k_2 in (A.1) are

$$k_j = \frac{C_{11}v_j - C_{44}}{C_{13} + C_{44}} = \frac{v_j(C_{13} + C_{44})}{C_{33} - v_j C_{44}}, \quad j = 1, 2. \tag{A.4}$$

In the case $v_1 \neq v_2$, representation (A.1) is general. A slightly modified, complex-valued form of general solution was suggested by Fabrikant (1989).

Now, we introduce new spatial variables $x_j = x$, $y_j = y$, $z_j = z/\sqrt{v_j}$; in these variables,

$$\left(\frac{\partial^2}{\partial x_j^2} + \frac{\partial^2}{\partial y_j^2} + \frac{\partial^2}{\partial z_j^2}\right)\Phi_j = 0. \tag{A.5}$$

The sets of singular and regular partial solutions are given by (A.1), with the potential functions

$$\begin{aligned} \Phi_{ts}^{(j)} &= \frac{1}{(2t+1)}[F_{t+1}^s(\mathbf{r}_j, d_j) - F_{t-1}^s(\mathbf{r}_j, d_j)], \\ \phi_{ts}^{(j)} &= \frac{1}{(2t+1)}[f_{t+1}^s(\mathbf{r}_j, d_j) + f_{t-1}^s(\mathbf{r}_j, d_j)], \\ t &= 0, 1, 2, \ldots, \quad |s| \leqslant t+1, \end{aligned} \tag{A.6}$$

where

$$\begin{aligned} F_t^s(\mathbf{r}, d) &= \frac{(t-s)!}{(t+s)!} Q_t^s(\xi) P_t^s(\eta) \exp(\mathrm{i}s\varphi), \\ f_t^s(\mathbf{r}, d) &= \frac{(t-s)!}{(t+s)!} P_t^s(\xi) P_t^s(\eta) \exp(\mathrm{i}s\varphi), \end{aligned} \tag{A.7}$$

are the singular and regular, respectively, harmonic functions obtained by separation of variables in the Laplace equation written in the spheroidal coordinates Hobson (1931), P_t^s and Q_t^s are the associated Legendre functions of the first and second kind, respectively. In (A.6), $(\xi_j, \eta_j, \varphi_j)$ for $v_j < 1$ are the modified prolate spheroidal coordinates

$$x + \mathrm{i}y = d_j \bar{\xi}_j \bar{\eta}_j \exp(\mathrm{i}\varphi_j), \quad z = \sqrt{v_j} z_j = \sqrt{v_j} d_j \xi_j \eta_j, \quad \bar{\xi}_j = \sqrt{(\xi_j)^2 - 1}, \quad \bar{\eta}_j = \sqrt{1 - (\eta_j)^2}. \tag{A.8}$$

In the case $v_j > 1$, one has to use the oblate spheroidal coordinates instead.

Note that, according to Hobson (1931), $F_t^s = f_t^s \equiv 0$ for $|\, s \,| > t$; this condition, however, makes it impossible to represent some of the singular solutions in the form (A.1) and (A.6). To resolve for this difficulty, we exploit the Podil'chuk's (1984) idea and introduce the following, additional to (A.7), functions of the form

$$F_t^{t+k}(\mathbf{r}, d) = \frac{1}{(2t+k)!} Q_t^{t+k}(\xi) P_t^{t+k}(\eta) \exp[\mathrm{i}(t+k)\varphi], \quad k = 0, 1, 2, \ldots, \tag{A.9}$$

where

$$P_t^{t+k}(p) = \frac{(2t+k)!}{(1-p^2)^{(t+k)/2}} \underbrace{\int_p^1 \int_p^1 \cdots \int_p^1}_{t+k} P_t(p)(\mathrm{d}p)^{t+k} = \frac{(2t+k)!}{(1-p^2)^{(t+k)/2}} I_{t+k}$$

for $0 \leqslant p \leqslant 1$; for $p < 0$, $P_t^{t+k}(p) = (-1)^k P_t^{t+k}(-p)$. We have for $k = 0$

$$I_t = \underbrace{\int_p^1 \int_p^1 \cdots \int_p^1}_{t} P_t(p)(\mathrm{d}p)^t = \frac{(1-p^2)^t}{2^t t!},$$

$$I_{t+1} = \int_p^1 I_t \,\mathrm{d}p = \frac{1}{2^t t!} \sum_{k=0}^{t} \frac{(-1)^k}{(2k+1)} \binom{n}{k} (1-p^{2k+1}),$$

$$I_{t+2} = \int_p^1 I_{t+1} \,\mathrm{d}p = \frac{1}{2^t t!} \sum_{k=0}^{t} \frac{(-1)^k}{(2k+1)} \binom{n}{k} \left[1 - p - \frac{(1-p^{2k+2})}{(2k+2)}\right], \text{ etc.}$$

It is fairly straightforward to show that the functions (A.9) are the singular solutions of the Laplace equations: unlike (A.7), they are discontinuous at $z = 0$. In the general series solution, however, these breaks cancel each other and give the continuous and differentiable expressions of the displacement and stress fields; for more discussion on this point, see Section 2. Note that the functions similar to F_t^{t+1} were used by Smith (1984) to solve the problem for a medium with a single penny-shape crack.

In (A.6), parameters of the modified spheroidal coordinate system (A.8) are chosen in a way that $\xi_j = \xi_{j0} = \text{const}$ at the surface $r = R$; i.e., S is the ξ-coordinate surface in each coordinate system introduced by (A.8). We provide this by defining

$$d_j = R/\xi_{j0}, \quad \xi_{j0} = \sqrt{\nu_j/|\nu_j - 1|}.$$

In this case, moreover, we have $\eta_j = \theta$ and $\varphi_j = \varphi$ for $r = R$, where (r, θ, φ) are the ordinary spherical coordinates corresponding to the Cartesian ones (x, y, z).

This is the key point: no matter how complicated solution in the bulk is, at the interface we get the linear combination of regular spherical harmonics $Y_t^s(\theta, \varphi) = P_t^s(\cos\theta)\exp(\mathrm{i}s\varphi)$. Under this circumstance, satisfaction the contact conditions at interface is the nothing more than standard algebra. Now, substituting $\phi_{ts}^{(j)}$ (A.6) into (A.1) and using the properties of the functions (A.7)

$$\begin{aligned}
&\frac{d}{(2t+1)}\left(\frac{\partial}{\partial x} - \mathrm{i}\frac{\partial}{\partial y}\right)[f_{t+1}^s(\mathbf{r}, d) + f_{t-1}^s(\mathbf{r}, d)] = f_t^{s-1}(\mathbf{r}, d),\\
&\frac{d}{(2t+1)}\left(\frac{\partial}{\partial x} + \mathrm{i}\frac{\partial}{\partial y}\right)[f_{t+1}^s(\mathbf{r}, d) + f_{t-1}^s(\mathbf{r}, d)] = -f_t^{s+1}(\mathbf{r}, d),\\
&\frac{d}{(2t+1)}\frac{\partial}{\partial z}[f_{t+1}^s(\mathbf{r}, d) + f_{t-1}^s(\mathbf{r}, d)] = f_t^s(\mathbf{r}, d),
\end{aligned} \tag{A.10}$$

we obtain the following set of regular vectorial solutions:

$$\begin{aligned}
&\mathbf{f}_{ts}^{(j)}(\mathbf{r}) = f_t^{s-1}(\mathbf{r}_j, d_j)\mathbf{e}_1 - f_t^{s+1}(\mathbf{r}_j, d_j)\mathbf{e}_2 + \frac{k_j}{\sqrt{\nu_j}} f_t^s(\mathbf{r}_j, d_j)\mathbf{e}_3, \quad j = 1, 2,\\
&\mathbf{f}_{ts}^{(3)}(\mathbf{r}) = f_t^{s-1}(\mathbf{r}_3, d_3)\mathbf{e}_1 + f_t^{s+1}(\mathbf{r}_3, d_3)\mathbf{e}_2, \quad t = 0, 1, 2, \ldots, \ |\, s \,| \leqslant t+1,
\end{aligned} \tag{A.11}$$

where the complex Cartesian basis vectors are $\mathbf{e}_1 = (\mathbf{e}_x + \mathrm{i}\mathbf{e}_y)/2$, $\mathbf{e}_2 = (\mathbf{e}_x - \mathrm{i}\mathbf{e}_y)/2$ and $\mathbf{e}_3 = \mathbf{e}_z$. In particular, $\mathbf{f}_{1s}^{(j)}$ describe linear deformation of the transversely isotropic solid

$$
\begin{aligned}
&2d_1\mathbf{f}_{10}^{(1)} = -x\mathbf{e}_x - y\mathbf{e}_y + 2\frac{k_1}{\nu_1}z\mathbf{e}_z,\\
&d_1(\mathbf{f}_{11}^{(1)} + \mathbf{f}_{1,-1}^{(1)}) = \frac{\mathrm{i}}{\sqrt{\nu_1}}(z\mathbf{e}_y + k_1 y\mathbf{e}_z),\\
&d_1(\mathbf{f}_{11}^{(1)} - \mathbf{f}_{1,-1}^{(1)}) = \frac{1}{\sqrt{\nu_1}}(z\mathbf{e}_x + k_1 x\mathbf{e}_z),\\
&2d_1(\mathbf{f}_{12}^{(1)} + \mathbf{f}_{1,-2}^{(1)}) = (x\mathbf{e}_x - y\mathbf{e}_y),\\
&2d_1(\mathbf{f}_{12}^{(1)} - \mathbf{f}_{1,-2}^{(1)}) = \mathrm{i}(x\mathbf{e}_y + y\mathbf{e}_x),\\
&2d_2\mathbf{f}_{10}^{(2)} = -x\mathbf{e}_x - y\mathbf{e}_y + 2\frac{k_2}{\nu_2}z\mathbf{e}_z,\\
&2d_3\mathbf{f}_{10}^{(3)} = \mathrm{i}(y\mathbf{e}_x - x\mathbf{e}_y), \quad d_3\left(\mathbf{f}_{11}^{(3)} + \mathbf{f}_{1,-1}^{(3)}\right) = \frac{1}{\sqrt{\nu_3}}z\mathbf{e}_x,\\
&d_3(\mathbf{f}_{11}^{(3)} - \mathbf{f}_{1,-1}^{(3)}) = \frac{\mathrm{i}}{\sqrt{\nu_3}}z\mathbf{e}_y,
\end{aligned}
\tag{A.12}
$$

the displacement vector $\mathbf{u}_0 = \hat{E}\cdot\mathbf{r}$ can be written as a linear combination of functions (A.12).

At the spherical surface $r = R$, the functions $\mathbf{f}_{ts}^{(j)}(\mathbf{r})$ (A.11) take the form

$$
\begin{aligned}
&\mathbf{f}_{ts}^{(j)}(\mathbf{r})\,|_S = P_t^{s-1}(\xi_{j0})\chi_t^{s-1}\mathbf{e}_1 - P_t^{s+1}(\xi_{j0})\chi_t^{s+1}\mathbf{e}_2 + \frac{k_j}{\sqrt{\nu_j}}P_t^s(\xi_{j0})\chi_t^s\mathbf{e}_3,\\
&\mathbf{f}_{ts}^{(3)}(\mathbf{r})\,|_S = P_t^{s-1}(\xi_{30})\chi_t^{s-1}\mathbf{e}_1 + P_t^{s+1}(\xi_{30})\chi_t^{s+1}\mathbf{e}_2,
\end{aligned}
\tag{A.13}
$$

where $\chi_t^s = \frac{(t-s)!}{(t+s)!}Y_t^s(\theta,\varphi)$, readily to be substituted in the interfacial boundary conditions (2) for displacements.

To satisfy the stress boundary conditions, we need the similar expressions for the traction vector $\mathbf{T}_\mathbf{n} = \sigma\cdot\mathbf{n}$. After somewhat involved algebra, we obtain the following representation of $\mathbf{T}_\mathbf{n}(\mathbf{f}_{ts}^{(j)})$ at the surface S:

$$
\begin{aligned}
\frac{d_j}{C_{44}}\mathbf{T}_\mathbf{n}(\mathbf{f}_{ts}^{(j)})\big|_S = {}&\frac{1}{\sqrt{\nu_j}}\left[(k_1+1)P_t'^{s-1}(\xi_{j0}) - \frac{(s-1)}{\xi_{j0}}\frac{(\nu_j C_{12} - k_j C_{13})}{\nu_j C_{44}}P_t^{s-1}(\xi_{j0})\right]\chi_t^{s-1}\mathbf{e}_1 - \frac{1}{\sqrt{\nu_j}}\left[(k_1+1)P_t'^{s+1}(\xi_{j0})\right.\\
&\left.+\frac{(s+1)}{\xi_{j0}}\frac{(\nu_j C_{12} - k_j C_{13})}{\nu_j C_{44}}P_t^{s+1}(\xi_{j0})\right]\chi_t^{s+1}\mathbf{e}_2 + (k_1+1)P_t'^{s}(\xi_{j0})\chi_t^s\mathbf{e}_3, \quad j = 1,2,
\end{aligned}
\tag{A.14}
$$

$$
\begin{aligned}
\frac{d_3}{C_{44}}\mathbf{T}_\mathbf{n}(\mathbf{f}_{ts}^{(3)})\big|_S = {}&\frac{1}{\sqrt{\nu_3}}\left[P_t'^{s-1}(\xi_{30}) + (s-1)\frac{\xi_{30}}{(\overline{\xi}_{30})^2}P_t^{s-1}(\xi_{30})\right]\chi_t^{s-1}\mathbf{e}_1\\
&+\frac{1}{\sqrt{\nu_3}}\left[P_t'^{s+1}(\xi_{30}) - (s+1)\frac{\xi_{30}}{(\overline{\xi}_{30})^2}P_t^{s+1}(\xi_{30})\right]\chi_t^{s+1}\mathbf{e}_2 + \frac{1}{\sqrt{\nu_3}}\frac{s}{\overline{\xi}_{30}}P_t^s(\xi_{30})\chi_t^s\mathbf{e}_3.
\end{aligned}
$$

The results exposed above imply $\nu_1 \neq \nu_2$. When $\nu_1 = \nu_2$, solution (A.1) is not general because of $\mathbf{f}_{ts}^{(1)} \equiv \mathbf{f}_{ts}^{(2)}$. In this case, however, the general solution of $\nabla\cdot\sigma = 0$ can be represented as

$$
\begin{aligned}
&u_x = \frac{\partial\Phi_1}{\partial x} + z\frac{\partial\Psi}{\partial x} + \frac{\partial\Phi_3}{\partial y}, \quad u_y = \frac{\partial\Phi_1}{\partial y} + z\frac{\partial\Psi}{\partial y} - \frac{\partial\Phi_3}{\partial x},\\
&u_z = \frac{\partial\Phi_1}{\partial z} + z\frac{\partial\Psi}{\partial z} - \frac{C_{13}+3C_{44}}{C_{13}+C_{44}}\Psi
\end{aligned}
\tag{A.15}
$$

or, in the vectorial form,

$$\mathbf{u} = \nabla\Phi_1 + \nabla\times(\Phi_3\mathbf{e}_z) + \left(z\nabla - \frac{C_{13}+3C_{44}}{C_{13}+C_{44}}\mathbf{e}_z\right)\Psi,$$

where the potential function Ψ satisfies Eq. (A.2) with $v = v_1$. To get the complete set of independent solutions (A.11), $\mathbf{f}_{ts}^{(2)}$ can be taken in the form

$$\mathbf{f}_{ts}^{(2)}(\mathbf{r}) = d_1\left(z\nabla - \frac{C_{13}+3C_{44}}{C_{13}+C_{44}}\mathbf{e}_z\right)f_t^s(\mathbf{r}_1,d_1) + \sqrt{v_1}d_1(\xi_{10})^2\nabla f_{t-1}^s(\mathbf{r}_1,d_1). \tag{A.16}$$

With the last term added, expression of $\mathbf{f}_{ts}^{(2)}$ at the surface $r = R$ is rather simple:

$$\begin{aligned}\mathbf{f}_{ts}^{(2)}(\mathbf{r})\mid_S = {}& \sqrt{v_1}\frac{\xi_{10}}{(t+s)}P_{t-1}^{s-1}(\xi_{10})\chi_t^{s-1}\mathbf{e}_1 - \sqrt{v_1}\frac{\xi_{10}}{(t+s+2)}P_{t-1}^{s+1}(\xi_{10})\chi_t^{s+1}\mathbf{e}_2\\ &+\left[\frac{\xi_{10}}{(t+s+1)}P_{t-1}^{s}(\xi_{10}) - \frac{C_{13}+3C_{44}}{C_{13}+C_{44}}P_t^s(\xi_{10})\right]\chi_t^s\mathbf{e}_3.\end{aligned} \tag{A.17}$$

For the expression of the corresponding traction vector, see Podil'chuk (1984).

The explicit form of the singular solutions $\mathbf{F}_{ts}^{(j)}$ is given by Eq. (A.11) with the replace f_t^s on F_t^s. To get the expression of $\mathbf{F}_{ts}^{(j)}$ and $\mathbf{T}_{\mathbf{n}}(\mathbf{F}_{ts}^{(j)})$ at the interface, one has to substitute $P_t^s(\xi)$ by $Q_t^s(\xi)$ in (A.13) and (A.14), respectively.

References

Bateman, G., Erdelyi, A., 1953. In: Higher Transcendental Functions, vol. 2. McGraw-Hill, New York.

Chen, H.S., Acrivos, A., 1978. The solution of the equations of linear elasticity for an infinite region containing two spherical inclusions. International Journal of Solids and Structures 14, 331–348.

Fabrikant, V.I., 1989. Applications of Potential Theory in Mechanics. Kluwer Academic, The Netherlands.

Hobson, E.W., 1931. The Theory of the Spherical and Ellipsoidal Functions. Cambridge University Press.

Hori, M., Nemat-Nasser, S., 1993. Double-inclusion model and overall moduli of multiphase composites. Mechanics of Materials 14, 189–206.

Iwakuma, T., Nemat-Nasser, S., 1983. Composites with periodic microstructure. Computers and Structures 16, 13–19.

Kushch, V.I., 1985. Elastic equilibrium of a medium containing periodic spherical inclusions. Soviet Applied Mechanics 21, 435–442.

Kushch, V.I., 1996. Elastic equilibrium of a medium containing finite number of aligned spheroidal inclusions. International Journal of Solids and Structures 33, 1175–1189.

Kushch, V.I., 1997a. Conductivity of a periodic particle composite with transversely isotropic phases. Proceedings of the Royal Society of London A 453, 65–76.

Kushch, V.I., 1997b. Microstresses and effective elastic moduli of a solid reinforced by periodically distributed spheroidal inclusions. International Journal of Solids and Structures 34, 1353–1366.

Kushch, V.I., Sangani, A., 2000. Conductivity of a composite containing uniformly oriented penny-shaped cracks or perfectly conducting inclusions. Proceedings of the Royal Society of London A 456, 683–699.

Kushch, V.I., Sevostianov, I., 2003. Effective elastic properties of the particulate composite with transversely isotropic phases. International Journal of Solids and Structures, submitted for publication.

Moskovidis, Z.A., Mura, T., 1975. Two ellipsoidal inhomogenities by the equivalent inclusion method. Journal of Applied Mechanics 42, 847–852.

Mura, T., 1982. Micromechanics of Defects in Solids. Martinus Nijhoff, The Hague, Netherlands.

Nunan, C.K., Keller, J.B., 1984. Effective elasticity tensor of a periodic composite. Journal of the Mechanics and Physics of Solids 32, 259–280.

Pan, Y.-C., Chou, T.W., 1976. Point force solution for an infinite transversely isotropic solid. Journal of Applied Mechanics 43, 608–612.

Podil'chuk, Yu.N., 1984. The Boundary Value Problems of Statics of Elastic Body. Naukova Dumka, Kiev (In Russian).

Podil'chuk, Yu.N., 2001. Exact analytical solutions of three-dimensional static thermoelastic problems for a transversely isotropic body in curvilinear coordinate systems. International Applied Mechanics 37 (6), 728–761.

Rodin, G.J., Hwang, Y.-L., 1991. On the problem of linear elasticity for an infinite region containing a finite number of non-intersecting spherical inhomogeneities. International Journal of Solids and Structures 27, 145–159.

Sangani, A.S., Lu, W., 1987. Elastic coefficients of composites containing spherical inclusions in a periodic array. Journal of the Mechanics and Physics of Solids 35, 1–21.

Smith, R.N.L., 1984. Stresses from arbitrary loads on a penny-shaped crack. International Journal for Numerical Methods in Engineering 20, 2093–2105.

Willis, J.R., 1975. The interactions of gas bubbles in an anisotropic elastic solid. Journal of the Mechanics and Physics of Solids 23, 129–138.

Withers, P.J., 1989. The determination of the elastic field of an ellipsoidal inclusion in a transversely isotropic medium, and its relevance to composite materials. Philosophical Magazine 59, 759–781.